Journal of Hydraulic Structures
J. Hydraul. Struct., 2022; 8(4):45-56
DOI: 10.22055/jhs.2023.42542.1237

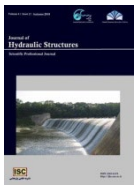

OPEN ACCESS

Numerical investigation of bed-load changes on sediment flushing cavity

Reza Nematzadeh [1]
Gholam Abbas Barani [1]
Ehsan Fadaei-Kermani [2]

Abstract

The tanks' useful life will be reduced if their sediments are not discharged with a suitable method. Various hydraulic and mechanical methods can be used in many countries to discharge sediments from reservoirs. Pressure hydraulic sediment flushing is a method of sediment flushing without lowering the water level. In the present study, using the CFD based Flow-3D software, a model has been applied to investigate the pressure hydraulic sediment flushing process, and evaluate the effect of blockage phenomenon on sediment flushing efficiency. Results were compared with the available laboratory model. The dimensions of the simulated tank were 2.5 x 1.3 x 1.5 m in length, width and height, respectively, the height of the bed load was 0.4 m, and the diameter of the sediment particles was 0.3 mm according to the laboratory conditions. The average relative error for the sediment flushing cone depth was about 3%. In addition, to investigate the blocking phenomenon, the height of the bed load was considered to be 0.41, 0.45 and 0.5 meters for each simulation. The simulation results showed that when the height of the bed load increases, there is the highest sediment flushing efficiency and more sediment can be removed from the bottom outlet.

Keywords: Hydraulic sediment flushing, Numerical model, Flow-3D, Bed load height, Sediment flushing efficiency.

Received: 26 December 2022; Accepted: 09 February 2023

1. Introduction

The dam construction disturbs the balance of incoming and outgoing sediments and prevents the transportation of sediments to oceans and lakes known as rivers [1]. More than 100 million tons of cubic meters were poured into the seas and oceans before constructing reservoirs equivalent to 26% of global sediments. Gradual deposition, construction low rate and construction of new

[1] Department of Civil Engineering, Faculty of Engineering, Shahid Bahonar University of Kerman, Kerman, Iran.
[2] Department of Civil Engineering, Faculty of Engineering, Shahid Bahonar University of Kerman, Kerman, Iran. Email: e.fadaei@uk.ac.ir **(Corresponding Author)**

reservoirs have decreased the storage volume in the reservoirs. The population growth also decreases storage. Due to deposition, many reservoirs are significantly losing their function. For example, according to the survey data published by the Central Water Commission of India in the last 100 years, 141 out of 243 large reservoirs have lost their storage volume due to sediment accumulation in the last 50 years [2]. Hydraulic structures such as dams interrupt the sediment transport continuity through natural rivers, which causes the sediments accumulation in the reservoir of the dam [3]. The tank's sediment discharge method is vital in removing or reducing the sediment and restoring the storage capacity. Water availability in rivers is seasonal and annual throughout the world [4]. There is insufficient water during droughts to meet human needs, Pressure hydraulic sediment flushing refers to removing accumulated sediments with hydraulic sediment removal techniques [5]. Hydraulic sediment flushing occurs when the water level in the bottom outlet is low, or the valve is opened for downstream uses. Due to erosion, the sediments deposited in the reservoir bed are detached and removed from the reservoir along with the water flow. After that, the sediment flushing cone is immediately observed by opening the bottom valve. On the other hand, the removal of sediments with this method is limited upstream of the bottom outlet, and the water height upstream is constant and stable[6,7]. In addition, the sediment flushing cone facing the bottom outlet is naturally developed with accumulated sediments [8,9]. (Figure 1). shows a schematic of pressure hydraulic sediment flushing and creating a sediment flushing cone in Brazil's Rio San Antonio dam reservoir [10].

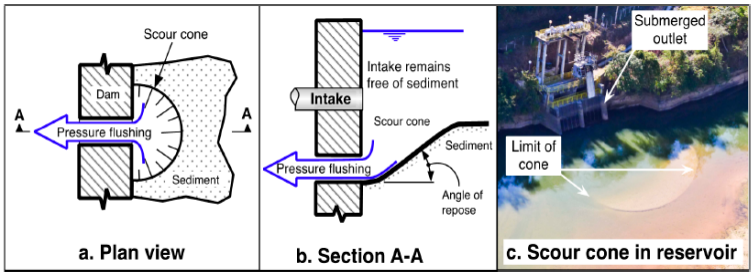

Figure 1. (a, b) Schematic of pressure hydraulic sediment flushing, c sediment washing cone created in Rio San Antonio dam reservoir, Brazil [10].

In recent years, issues related to sediment flushing have been numerically and experimentally studied in many countries, among which the following can be mentioned. Shen et al. proposed a dimensionless and regression relationship using laboratory and field data to estimate the depth of the chassis cone in non-cohesive sediments and pressure chassis conditions [11]. Ahadpour et al. experimentally investigated a new idea in pressure sediment flushing. Their study investigated the use of vibrators in sedimentary layers and their location on the dimensions of the sediment flushing hole and its volume. Their results show that a vibrator inside the sediments behind the tank positively affects the dimensions of the sediment flushing hole. In addition, the position of the vibrator to the ox dam and the vibrator's frequency are the main parameters affecting the dimensions of the sediment flushing hole [12]. Altus et al. investigated the effect of a swirling flow produced by four jets to suspend the suspended sediments inside the tank so that the sediments are removed through the bottom outlet before settling in the tank. They investigated the effect of geometrical parameters of the bottom outlet, flow pattern and jet flow discharge on sediment discharge efficiency. Finally, They suggested the best strategy to produce the highest discharge efficiency [13]. Haghjouei et al. investigated the effects of vortices caused by pressure changes in the entrance to the structure, both sides, and in the exit area of the bottom outlet using

a physical and structural model with a new structural configuration with the ability to drain in a straight path and on both sides of the tank with angles of 30, 45 and 60 degrees .Experiments were performed on three flow discharge and three-bed load heights, and non-cohesive and coarse-grained sediments were used. The results showed that the use of this structure positively affected the volume and dimensions of the sediment flushing cone. Finally, the statistical analysis of the results developed a dimensionless equation to calculate the dimensions of the sediment discharge cone for the characteristics of the sediment tested [14,15]. Pressure flushing can greatly improve the efficiency of dams and power plants [16]. It can also be an effective mechanism for removing sediments, draining the reservoir through low-level outlets and allowing natural flows to remove sediments. To investigate the effects of submerged vane placement on the performance of hydraulic flushing, Beiramipour et al. used the submerged vanes with convergent, divergent, and combined arrangements at three distances of the vanes from the bottom discharging outlet, and three distances between the vanes with three different heights. Compared with the no-structure test, the results indicated that using the submerged vanes with convergent and divergent arrangements increased the volume of discharged sediments by 48 times, while using two-row combined vanes in divergent arrangements increased the flushing pit by 51 times of load bearing compared to the control test [17].

Due to the importance of pressure hydraulic sediment flushing, this paper deals with the numerical modeling of this process to investigates the flow and discharge of sediments and simulation of the Chassis cone using the Flow-3D numerical model. The results of pressure hydraulic sediment flushing have been compared with the laboratory results, and the model validation was conducted. In addition, this study provides a solution to increase sediment flushing efficiency by using computational fluid dynamics software and investigates the parameters involved in this phenomenon.

2. Materials and method

Flow-3D software provides engineers solutions for simulating the flow of liquids and gases in various industrial applications and physical processes. This software is popular due to its good performance in time-dependent modeling problems and flows in contact with the free surface of the fluid in one, two and three dimensions, but it can also handle limited and stable flows. The dimensions of the main flume of the channel are in the form of a rectangular cube with a length, width and height of 2.5, 1.3 and 1.5 meters, respectively. The drain pipe is one meter long and has a diameter of 9.5 cm. The flow is directed to a calibrated sharp-edged triangular weir after passing through the sediment settling basin, and the flow discharge is measured with this weir. Finally, the water is directed again to the underground tank (water supply system) after passing through this weir. A valve can adjust the inlet flow to the tank. A triangular weir with a vertex angle of 90 degrees was installed at the end of the second sedimentation basin to measure the output flow [7]. The first sediment settling tank and the second tank are also one meter long.Sediments are non-cohesive and sandy. The average diameter of sediment particles is 0.3 mm, and the density of particles is 1800 kg/m3. The inlet flow to the tank is stable and permanent, and there will be no phreatic decline in the tank over time. The tools prepared in the bilingual Meshing & Geometry software have been used to create the geometry of the laboratory model. (Figure 2). shows a schematic diagram of the tank.

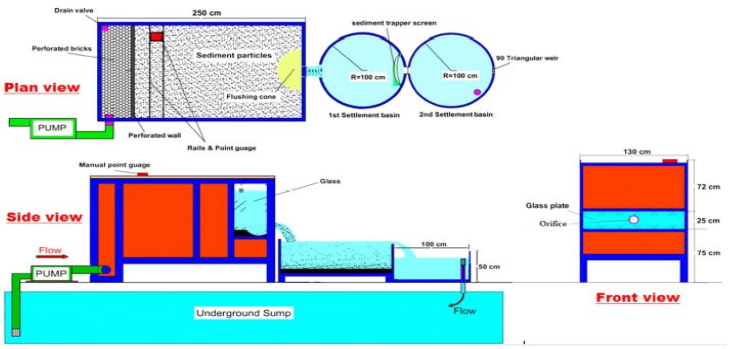

Figure 2. Schematic of the laboratory flume

2.1. Flow-3D numerical model equations

The fluid flow equations are obtained from the law of conservation of mass and momentum and are partial differential equations. The main equations for 3D flow simulation are three differential equations, including continuity equations and the amount of movement in the x, y, z direction.

2.1.1. continuity equation

The flow continuity equation is obtained from the law of conservation of mass and by writing the balanced equation for a fluid element. The continuity equation is as follows:

$$v_f \frac{\delta f}{\delta t} + \frac{\delta}{\delta x}(\rho u A_x \frac{\delta}{\delta z} \frac{\delta}{\delta y}(\rho v A_y) +) + (\rho w A_z)\xi \frac{\rho u A_x}{x} = R_{DIF} + R_{SOR} \quad (1)$$

where v_f is open volume fraction to flow, p is the fluid density, R_{DIF} is the turbulence diffusion term and R_{SOR} is the mass source. The velocity components are (u, v, w) in the (x, y, z) directions. A_x is the open surface fraction in the x direction. A_y and A_z are similarly the surface fraction in the y and z directions [18].

2.1.2. The equation of momentum

Fluid motion equations with velocity components (u, v, w) in three coordinate directions, i.e., Navier-Stokes equations, are as follows:

$$\frac{\delta u}{\delta t} + \frac{1}{v_f}(uA_x \frac{\delta u}{\delta x} + vA_y \frac{\delta u}{\delta y} + wA_z \frac{\delta u}{\delta z}) = -\frac{1}{\rho} \frac{\delta p}{\delta x} + G_x + f_x \quad (2)$$

$$\frac{\delta v}{\delta t} + \frac{1}{v_f}(uA_x \frac{\delta v}{\delta x} + vA_y \frac{\delta v}{\delta y} + wA_z \frac{\delta v}{\delta z}) = -\frac{1}{\rho} \frac{\delta p}{\delta y} + G_y + f_y \quad (3)$$

$$\frac{\delta w}{\delta t} + \frac{1}{v_f}(uA_x \frac{\delta w}{\delta x} + vA_y \frac{\delta w}{\delta y} + wA_z \frac{\delta w}{\delta z}) = -\frac{1}{\rho} \frac{\delta p}{\delta z} + G_z + f_z \quad (4)$$

In these equations, (G_x, G_y, G_z) are the terms of mass acceleration, and (f_x, f_y, f_z) are the terms of viscosity acceleration. The transport equation of any i-th types of suspended sediments is as follows without considering the functions:

$$\frac{\partial c_{si}}{\partial t} + \nabla \cdot (\bar{u} c_{si}) = 0 \quad (5)$$

Where C_{si} is the concentration of suspended sediment in unit mass per unit volume, and $\bar{u}$ is the average velocity of sediment and fluid mixture.

The density of sediments is higher than the surrounding fluid; therefore, the sediment particles will be deflected inside the fluid. The intensity of this deviation depends on the balance between buoyant and drag forces. Therefore, it is possible to write the momentum balance relation for each sediment particle and fluid-sediment mixture:

$$\frac{\partial u_{si}}{\partial t} + \bar{u} \cdot \nabla u_{si} = -\frac{1}{\rho_{si}} \nabla p + F - \frac{K_i}{f_{si} \rho_{s'}} \cdot u_{ri} \quad (6)$$

$$\frac{\partial \bar{u}}{\partial t} + \bar{u} \cdot \nabla \bar{u} = -\frac{1}{\rho} \nabla p + F \quad (7)$$

Where u_{si} is the velocity of the i-th types of sedimentary particles, ρ_{si} is the density of sedimentary materials, f_{si} is the volume fraction of the i-th species of sedimentary particles, P is the pressure, K is the drag function, F is the sum of the volumetric force and the viscous force, and u_{ri} is the relative velocity which is obtained from the following relation:

$$u_{ri} = u_{si} - u_f \quad (8)$$

The average speed can also be used from the following relationship:

$$\bar{u} = [1 - \sum_{i=1}^{n} f_{si}] u_f + \sum_{i=1}^{n} f_{si} u_{si} \quad (9)$$

Where n is the total number of types of sediment particles, the following result is obtained by subtracting equation (6) from equation (7):

$$\frac{\partial u_{drift,i}}{\partial t} + \bar{u} \cdot \nabla_{u_{drift,i}} = \left[\frac{1}{\bar{\rho}} - \frac{1}{\rho_{s,i}}\right] \nabla P - \frac{K_i}{f_{s,i} \rho_{s,i}} u_{r,i} \quad (10)$$

Such that $u_{drift,i} = u_{s,i} - \bar{u}$ represents Drift Velocity. This velocity is used to measure sediment deflection. This velocity is calculated assuming that each sediment particle moves independently from other particles. This equation will be rewritten with this assumption that sediments' movement is almost constant at the computational time scale and movement term has minor change (i.e., for low drift velocity):

$$u_{r,i} = \frac{\nabla P}{\bar{\rho} K_i} (\rho_{s,i} - \tilde{\rho}) f_{s,i} \quad (11)$$

The average density of the fluid-sediment mixture ($\bar{\rho}$) is measured as follows:

$$\bar{\rho} = \left[1 - \sum_{i=1}^{n} f_{s,i}\right] \rho_f + \sum_{i=1}^{n} f_{s,i} \beta_{s,i} \quad (12)$$

It should be noted that pressure gradient can have many oscillations in most simulations, especially near the free surface. In most cases, the ratio or pressure gradient to mixed density usually equals gravitational acceleration (g). The following equation can be written based on the mentioned assumption:

$$u_{r,i} = \frac{g}{K_i}(\rho_{s,i} - \bar{\rho})f_{s,i} \tag{13}$$

A reasonable choice for drag function K_i includes a combination of form drag and stokes drag:

$$K_i = \frac{3}{4}\frac{f_{s,i}}{d_{s,i}}\left[C_{D,i}\|u_{r,i}\| + 24\frac{\mu_f}{\rho_f d_{s,i}}\right] \tag{14}$$

where d_{Si} and C_{Di} indicate the diameter and coefficient of drag related to type i of sediment particles, and μ_f represents fluid viscosity. Finally, drift velocity is calculated using relative velocity. Regarding definitions of relative and drift velocities:

$$u_{drift,i} = (1 - f_{s,i})u_{r,i} - \sum_{j=1}^{n(-i)} f_{s,j}u_{r,j} \tag{15}$$

Five turbulence models are used in Flow-3D software: Prandtl mixing-length model, one-equation, turbulent energy model, two equation (k-e) model, renormalized group (RNG) model and a large eddy simulation model. In this simulation, two disturbance models, RNG and K-e, were used with acceptable results in the simulation of sedimentation in reservoirs. The RNG model was chosen among these two turbulence models due to its higher speed in reaching convergence and being more economical. This model was used in all simulation stages [19,20].

3. Numerical modeling of pressure hydraulic sediment flushing

It is essential to determine the appropriate boundary conditions in numerical models according to the type of flow and problem conditions. In addition, the initial condition can be a fluid-filled area inside the solution network when starting the simulation. In this simulation, the water height was 50 cm higher than the upper edge of the bottom outlet using the data and laboratory conditions and the sub-branch of Fluid Regions in the numerical model. In the simulation, the nested block method was used for the bottom outlet channel to optimally use the solution network. For the inlet flow, the boundary conditions of the specified pressure and digital elevation of water level were considered 1.1 m according to the laboratory conditions and the water height inside the tank. The outflow boundary condition was selected at the outlet flow's downstream boundary. The boundary condition for the tank wall was considered free space or symmetric. The floor of the solution domain was used from the boundary condition of the walls, and the ceiling of the block was used from the boundary condition of the specified pressure. The value of digital elevation was zero. In addition, due to the symmetry property, the boundary condition for all faces of the valve was considered free space or symmetry. (Figure 3). shows the boundary conditions applied in the simulation.

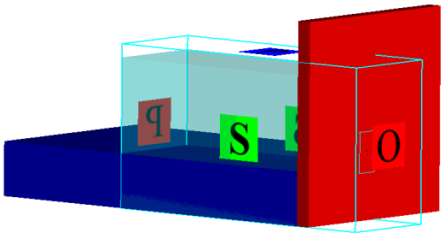

Figure 3. Boundary conditions applied in the simulation

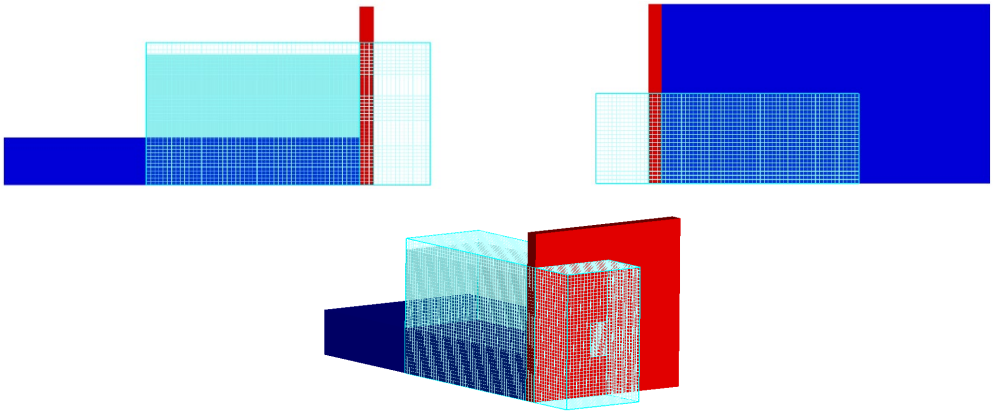

Figure 4. mesh view (a) profile (b) laboratory model plan (c) side view

Various mesh blocks with different dimensions have been used to analyze the numerical model's sensitivity. Finally, the best type of network was selected to continue the modeling process after checking the accuracy, error rate, and calculation time. After completing the simulation of the models with different dimensions of meshing and taking a few points from different directions of the chassis cone results from the laboratory results, the simulation results were compared with the results of the laboratory model. Type 3 meshing was selected as the best type for sensitivity analysis by taking different points. In addition, the average relative error for each meshing was separately calculated. Type 3 meshing has the lowest error percentage, therefore, it was used to continue the simulation process. The specifications of each meshing are shown in Table 1. (Figure 5). shows the result obtained from the numerical model with the corresponding values of the laboratory model for each of the grids.

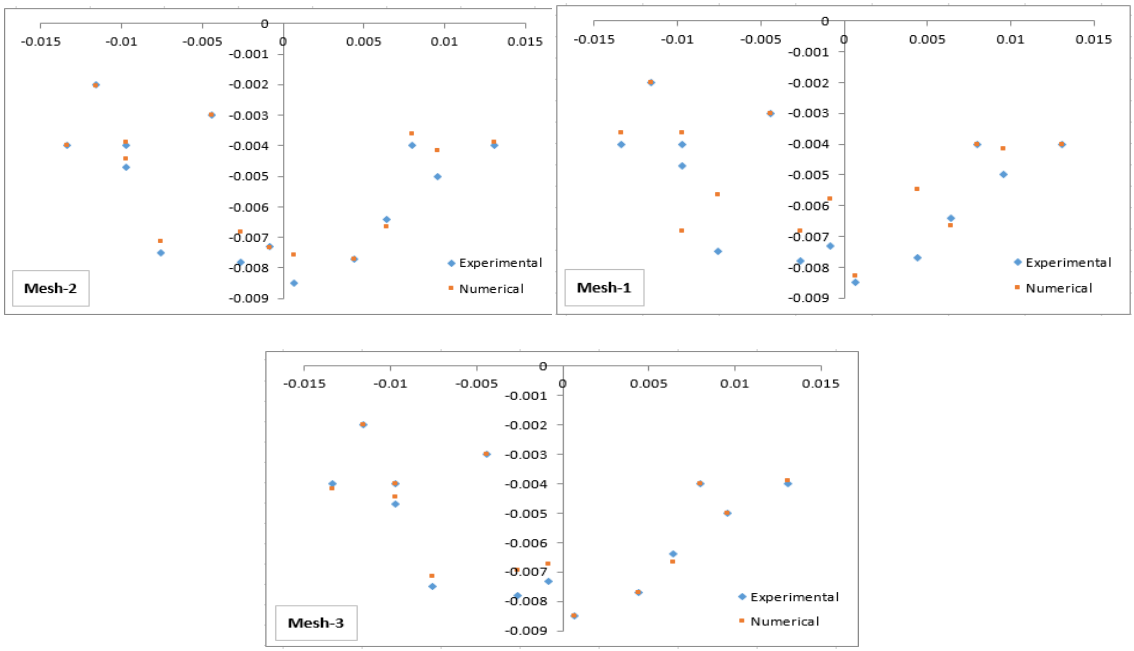

Figure 5. Comparison of experimental and numerical model results with different meshing

Table 1. specifications of computing grid meshing

Mesh type	Mesh dimensions	Average relative error	Calculation time
Type 1	0.06 m and 0.04 m	13.77	1:14:05
Type 2	0.02 m and 0.03 m	5.68	2:44:21
Type 3	0.03 m and 0.01 m	3.03	2:42:25

4. Results and discussion

In the following, the effect of increasing the height of the bed load (blockage phenomenon) on the efficiency of the pressure chassis operation was investigated after applying the appropriate boundary condition and carrying out the simulation and verification of modeling. For this purpose, 6 types of sediment layers with different heights were used to perform the simulation process and check the number of changes in the sediment flushing process. The bed load height was considered 410 mm in the first simulation. Then, Tecplot software was used as a counter to observe the results more precisely. Then, the simulation for the bed load with heights of 420, 430, 440, 450 and 500 mm was also investigated. According to the simulation results, when the blockage phenomenon and bed load height increase, the flow and sediment interaction and shear stress increase. This increase in shear stress increased the concentration of sediments around the bottom outlet area, increasing the efficiency of pressure hydraulic sediment flushing. (Figure 8). shows the changes in the pressure profile and the depth of the chassis cone for the bed load at the height of 410 mm. (Figure 9). shows the changes in the pressure profile and the depth of the chassis cone for the bed load at the height of 450 mm. In addition, (Figure 10) shows the changes in the pressure profile and the depth of the chassis cone for the bed load at the height of 500 mm. According to the results, the average relative error for the sediment flushing cone depth was obtained about 3% compared with the experimental data. Finally, figures 11 and 12 indicate the effect of sediment particles'

diameter on the sediment flushing process with particle diameters of 0.2 and 0.8mm, respectively.

Table 2. specifications and number of tests related to the bed layer

	Bed load height (m)	water height (m)	discharge (Lit/s)	Sediment particle diameter (mm)	Density of sediment particles (kg/m3)	Water temperature (C°)	Number of experiments
Simulation 1	0.41	1.1	5.14	0.3	1800	20	1
Simulation 2	0.45	1.1	5.14	0.3	1800	20	1
Simulation 3	0.50	1.1	5.14	0.3	1800	20	1

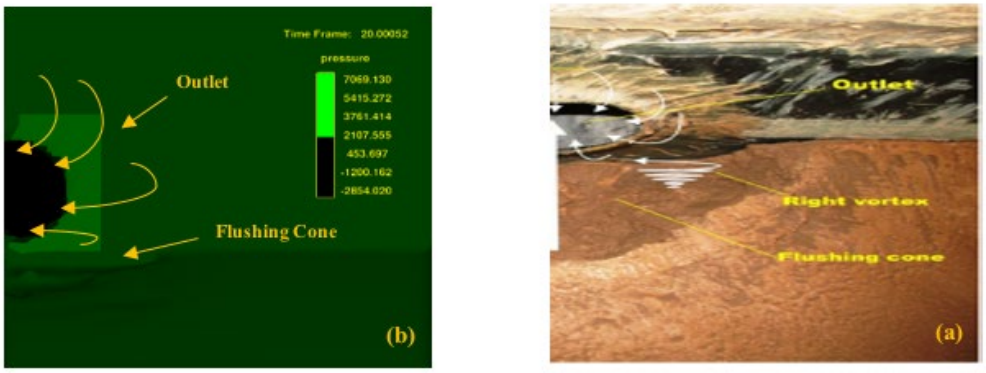

Figure 6. changes in the sediment flushing depth in the laboratory model (a) and the simulation process (b)

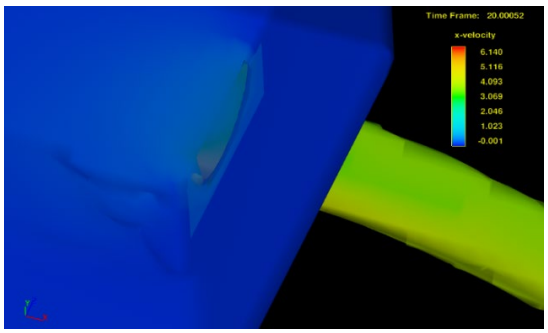

Figure 7. speed profile changes in the simulation process

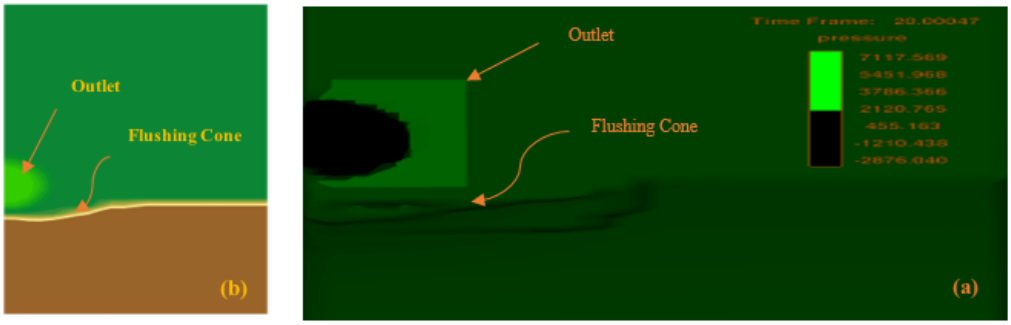

Figure 8. changes in the pressure profile (a) and the depth of the chassis cone (b) for the bed load at the height of 410 mm in the simulation process

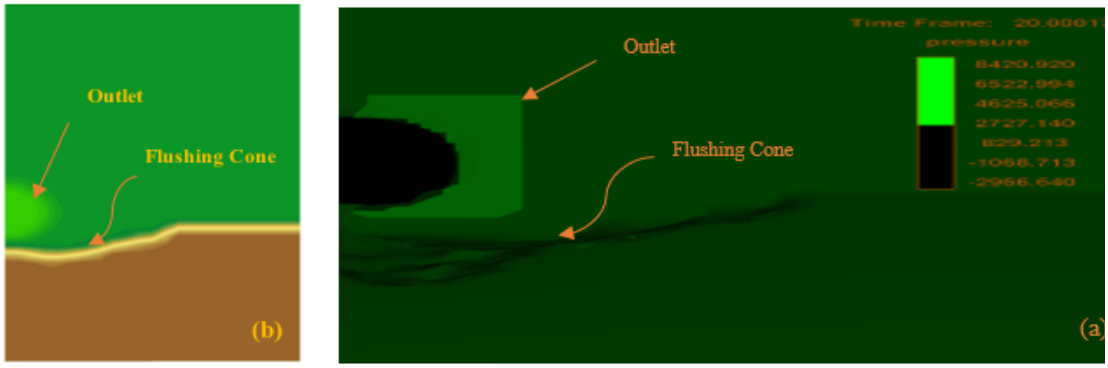

Figure 9. changes in the pressure profile (a) and the depth of the chassis cone (b) for the bed load at the height of 450 mm in the simulation process

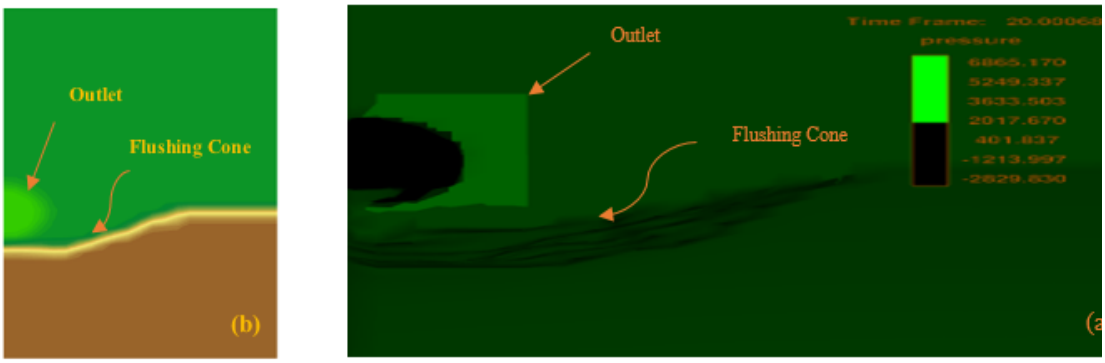

Figure 10. changes in the pressure profile (a) and the depth of the chassis cone (b) for the bed load at the height of 500 mm in the simulation process

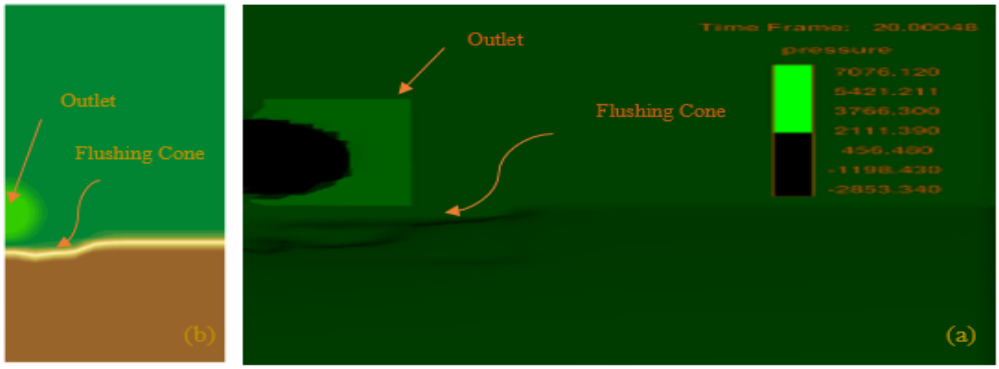

Figure 11. Changes in the pressure profile (a) and the depth of the chassis cone (b) For sediment particles with 0.2mm diameter

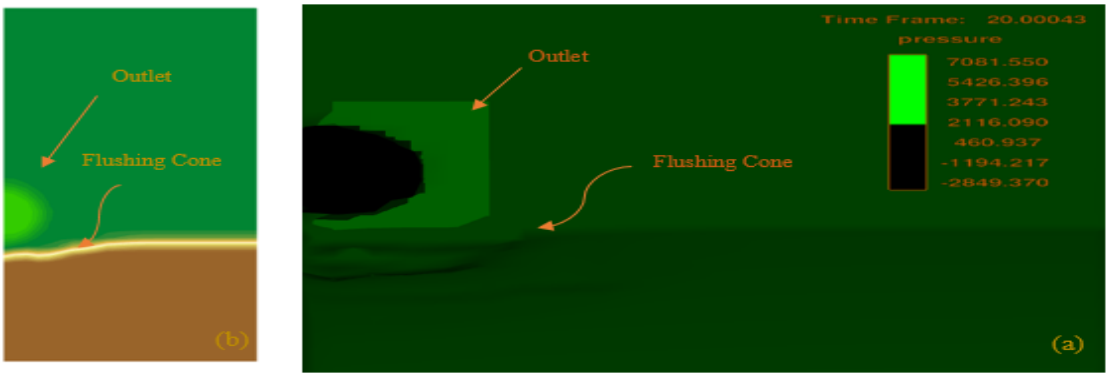

Figure 12. Changes in the pressure profile (a) and the depth of the chassis cone (b) For sediment particles with 0.8mm diameter

5. Conclusion

In the present study, the effect of blocking phenomenon on the efficiency of the pressure hydraulic sediment flushing process has been numerically investigated. The numerical simulation was applied according to the available laboratory model. The height of the bed load was considered 410, 420, 430, 440 and 500 mm for each simulation. The numerical model results showed that the increase in the blocking phenomenon had a positive and noticeable effect on the hydraulic sediment flushing efficiency. In addition, the increase in the amount of blocking (at least up to the level of the highest height of the bottom outlet edge) increases the dimensions of the sediment flushing cone. Moreover, the level of bed sediments showed that the most bed changes and sediment flushing occurred near the bottom outlet. According to limitation of pressure descaling around the bottom outlet valve, a river flow should be created to develop and expand the sediment flushing hole and discharge a larger volume of sediments into the tank.

References

1. Basson, G., and Bosman. E,. (2019). Flushig of sediments at hydropower plant dams. https://www.researchgate.net/publlcation/336676868.
2. AUEL, C, (2018). Sediment Bypassing – A Sustainable and Eco – Friendly Strategy Against Reservoir Sedimentation. Hydropower, Dam and River Engineering, ILF Consulting Engineering.
3. de Jalón, D. G., Bussettini, M., Rinaldi, M., Grant, G., Friberg, N., Cowx, I. G., & Buijse, T. (2017). Linking environmental flows to sediment dynamics. *Water Policy*, *19*(2), 358-375..
4. Haghjouei, H., Kantoush, S. A., Beiramipour, S., Rahimpour, M., & Qaderi, K. (2022). Experimental Study Demonstrating a Cost-Effective Approach for Generating 3D-Enhanced Models of Sediment Flushing Cones Using Model-Based SFM Photogrammetry. *Water*, *14*(10), 1588..
5. Malavoi, J.R. and El Kadi Abderrezzak, K., (2019). Reservoir Sedimentation dam safety and hydropower production: Hazards, risks and issues..
6. Castillo, L. G., Carrillo, J. M., & Álvarez, M. A. (2015). Complementary methods for determining the sedimentation and flushing in a reservoir. *Journal of Hydraulic Engineering*, *141*(11), 05015004.

7. Madadi, M. R., Rahimpour, M., & Qaderi, K. (2017). Improving the pressurized flushing efficiency in reservoirs: an experimental study. *Water Resources Management*, *31*(14), 4633-4647.
8. Khakzad, H., & Ivanovich Elfimov, V. (2015). Estimate of time required for environmentally friendly flushing in Dez dam reservoir. *Water Practice and Technology*, *10*(1), 73-85.
9. Annandale, G. W., Morris, G. L., & Karki, P. (2016). Extending the life of reservoirs: sustainable sediment management for dams and run-of-river hydropower. The World Bank.
10. Morris, G. L. (2020). Classification of management alternatives to combat reservoir sedimentation. *Water*, *12*(3), 861.
11. Kantoush, S. A., & Sumi, T. (2016). The aging of Japan's dams: Innovative technologies for improving dams water and sediment management. In *River Sedimentation* (pp. 1030-1037). CRC Press.
12. Dodaran, A. A., Park, S. K., Mardashti, A., & Noshadi, M. (2012). Investigation of dimension changes in under pressure hydraulic sediment flushing cavity of storage dams under effect of localized vibrations in sediment layers. *International Journal of Ocean System Engineering*, *2*(2), 71-81.
13. Jenzer Althaus, J. M., Cesare, G. D., & Schleiss, A. J. (2015). Sediment evacuation from reservoirs through intakes by jet-induced flow. *Journal of Hydraulic Engineering*, *141*(2), 04014078.
14. Haghjouei, H., Rahimpour, M., Qaderi, K., & Kantoush, S. A. (2021). Experimental study on the effect of bottomless structure in front of a bottom outlet on a sediment flushing cone. *International Journal of Sediment Research*, *36*(3), 335-347.
15. Emamgholizadeh, S., & Fathi-Moghdam, M. (2014). Pressure flushing of cohesive sediment in large dam reservoirs. *Journal of Hydrologic Engineering*, *19*(4), 674-681.
16. Esmaeili, T., Sumi, T., Kantoush, S. A., Kubota, Y., Haun, S., & Rüther, N. (2021). Numerical Study of Discharge Adjustment Effects on Reservoir Morphodynamics and Flushing Efficiency: An Outlook for the Unazuki Reservoir, Japan. *Water*, *13*(12), 1624.
17. Beiramipour, S., Qaderi, K., Rahimpour, M., Ahmadi, M. M., & Kantoush, S. A. (2021). Effect of submerged vanes in front of circular reservoir intake on sediment flushing cone. In *Proceedings of the Institution of Civil Engineers-Water Management* (Vol. 174, No. 5, pp. 252-266). Thomas Telford Ltd.
18. Hussain, K., & Shahab, M. (2020). Sustainable sediment management in a reservoir through flushing using HEC-RAS model: case study of Thakot Hydropower Project (D-3) on the Indus River. *Water Supply*, *20*(2), 448-458.
19. Flow Science, I. (2017). FLOW 3D User Manual.
20. Fadaei-Kermani, E. and Barani, G.A. (2014). Numerical simulation of flow over spillway based on the CFD method. Scientia Iranica. Transaction A, Civil Engineering, 21(1), 91.